Electronic Supplementary Information (ESI)

Colloidal quantum dot photonic crystal phosphor: nanostructural engineering of phosphor for enhanced color conversion

Kyungtaek Min,[a,b] Hyunho Jung,[b,c] Yeonsang Park,[d] Kyung-Sang Cho,[d] Young-Geun Roh,[d] Sung Woo Hwang,[d] and Heonsu Jeon[*b,c]

[a] Department of Energy Systems Research, Ajou University, Suwon 16499, Republic of Korea

[b] Inter-university Semiconductor Research Center, Seoul National University, Seoul 08826, Republic of Korea

[c] Department of Physics and Astronomy, Seoul National University, Seoul 08826, Republic of Korea

[d] Samsung Advanced Institute of Technology, Suwon 16678, Republic of Korea

[*]To whom correspondence should be addressed. E-mail: hsjeon@snu.ac.kr

Comparison of the amounts of CQDs in the PhC and reference phosphors.

The amounts of CQDs are estimated from the areas that the CQDs cover in the cross-sectional SEM images of the two kinds of phosphor samples, which is accomplished by counting the numbers of pixels for the appropriate areas in the corresponding SEM images. The numbers of pixels within the CQD-filled area in one unit cell are 2,424 pixels for the PhC phosphor and 2,464 pixels for the reference phosphor, respectively, which results in the ratio of 0.984:1 ≈ 1:1.

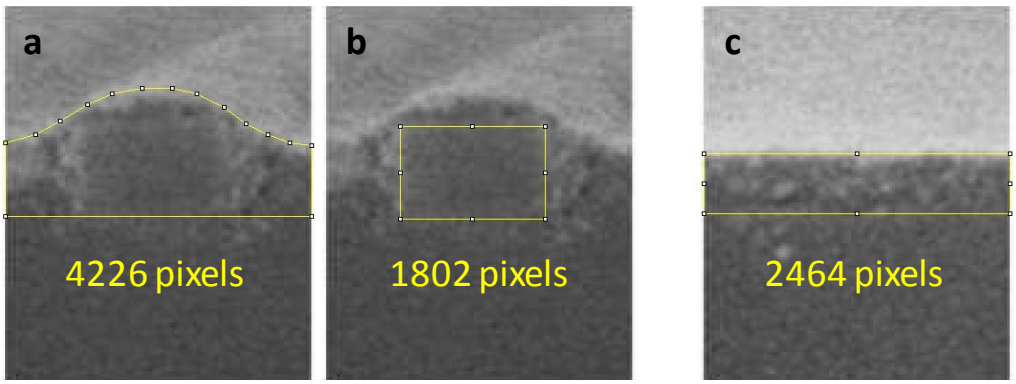

Fig. S1 SEM images of the unit cells of (a,b) the PhC phosphor and (c) the reference phosphor. The number of pixels indicated in each figure corresponds to the closed area defined by the yellow lines.

Enhanced CQD fluorescence via emission resonance

Besides the CQD fluorescence enhancement via the excitation resonance (between excitation photons and PBE modes), another resonance is still possible between photons emitted from CQDs and a propagating PhC mode,[1,2] which here we call the 'emission resonance' to distinguish it from the excitation resonance. The emission resonance can produce an additional enhancement in fluorescence through efficient extraction of photons. In fact, the emission resonance condition is already denoted in Fig. 2a in the main manuscript, where the CQD emission photon energy intersects a PhC band above the light-line. The CQD emission then becomes efficient via the leaky PhC mode at a particular radiation angle given by $\theta_{em} = sin^{-1}\left(k_x/k_{em}\right)$, where k_{em} is the wavenumber of photons emitted from CQDs.

For experimental confirmation, we measured far-field radiation patterns. To facilitate the measurements, we employed a compact 405 nm laser diode for CQD excitation; the excitation resonance for 405 nm can be achieved at the incidence angle of $\theta_{ex} \approx 12.5°$ (see Fig. 4d). Figs. S2a and b present far-field radiation patterns measured with $\theta_{ex} = 12.5°$ and $\theta_{ex} = 4°$, which represent the "on" and "off" excitation resonances, respectively. One can see from the upper panel of Fig. S2a that CQD emission from the PhC phosphor is largely enhanced at the emission resonance angle of $\theta_{em} \approx 38°$ (by a factor of ~3.5 when compared with the emission intensity at $\theta_{em} \approx 0°$). Note that this enhancement via the emission resonance is in addition to the global (regardless of emission angle) fluorescence enhancement via the excitation resonance (lower panel, Fig. S2a). In the "off" excitation resonance situation of $\theta_{ex} = 4°$, on the other hand, there is no global fluorescence enhancement, but the emission resonance at $\theta_{em} = 38°$ still occurs with the total fluorescence enhancement of ~3.5 (Fig. S2b). Fig. S2c presents fluorescence spectra from

the CQD PhC phosphor, recorded under the excitation resonance condition (θ_{ex} = 12.5°) but at a few different emission angles in vicinity of the emission resonance (θ_{em} = 38°). In huge contrast to the situation of *excitation resonance only* (Figs. 3a and 3b), where the spectral shapes remain unchanged, here a relatively sharp emission resonance peak moves across the broad CQD emission background as the emission (or detection) angle changes, with the maximum intensity at θ_{em} = 38°.

In order to help readers understand the differences between the excitation and emission resonances, we took some photograph images. Fig. S3 shows the images of CQD emission from both the PhC and reference phosphors, all taken at the emission resonance angle of θ_{em} = 38°. These images were taken with the previous wavelength-tunable source (instead of the compact 405 nm LD) because here we only need to take photographs at a fixed emission angle. Four images are arranged in a 2×2 matrix format: the PhC and reference phosphors are placed in the left and right columns while the "on" (λ_{ex} = 454 nm) and "off" (λ_{ex} = 480 nm) excitation resonance conditions are arranged in the top and bottom rows. It is clear that the PhC phosphor exhibits stronger emission intensity than the reference phosphor for the both excitation wavelengths because all the images are taken at the emission resonance condition. However, the strongest CQD emission comes when the both resonances (in excitation and emission) are satisfied: that is, from the PhC phosphor when excited resonantly.

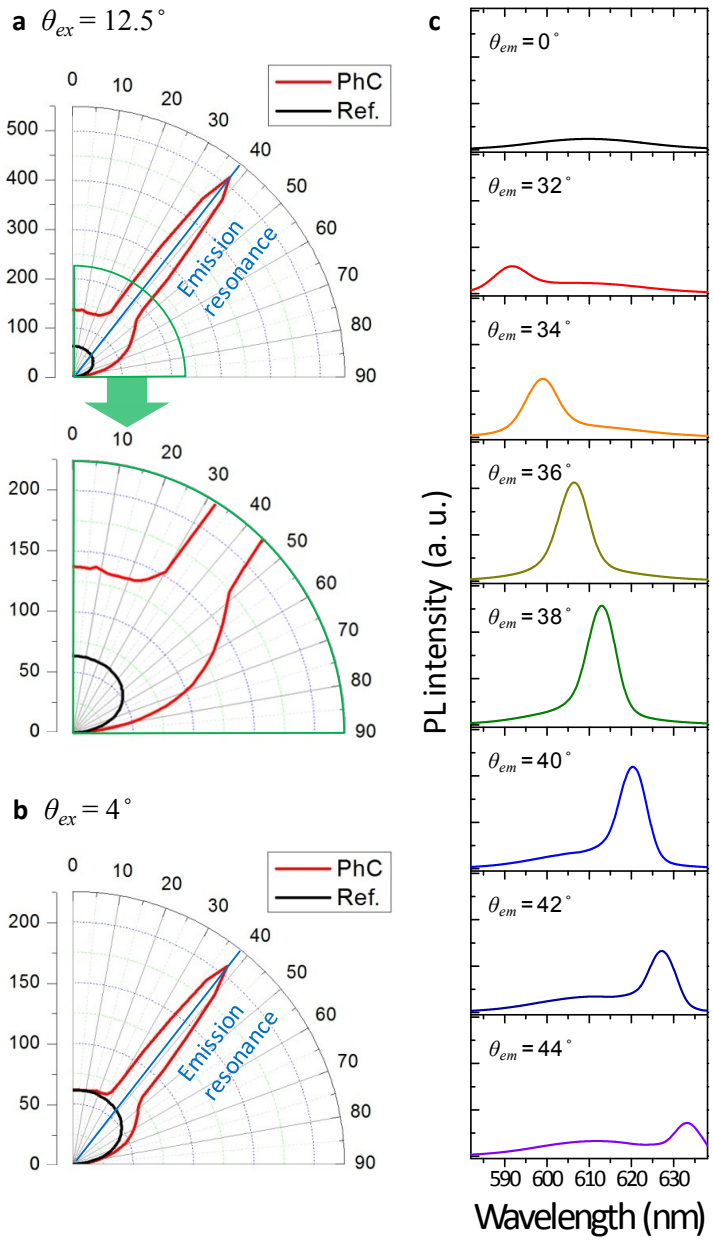

Fig. S2 Far-field emission patterns. (a) Integrated CQD emission intensity plotted as a function of emission (or detection) angle for the PhC phosphor (red) and the reference phosphor (black) measured at θ_{ex} = 12.5°, the "on-resonant" excitation condition for 405 nm. The lower panel is an amplification for the region outlined by the green lines in the upper panel. (b) Repeat of (a), but measured at θ_{ex} = 4°, an "off-resonant" excitation condition for 405 nm. Note that the intensity scale in Fig. S2b is the same as that of the lower panel of Fig. S2a. (c) CQD fluorescence spectra from the PhC phosphor under the excitation resonance condition (θ_{ex} = 12.5°), measured at different far-field emission angles near the emission resonance (θ_{em} = 38°).

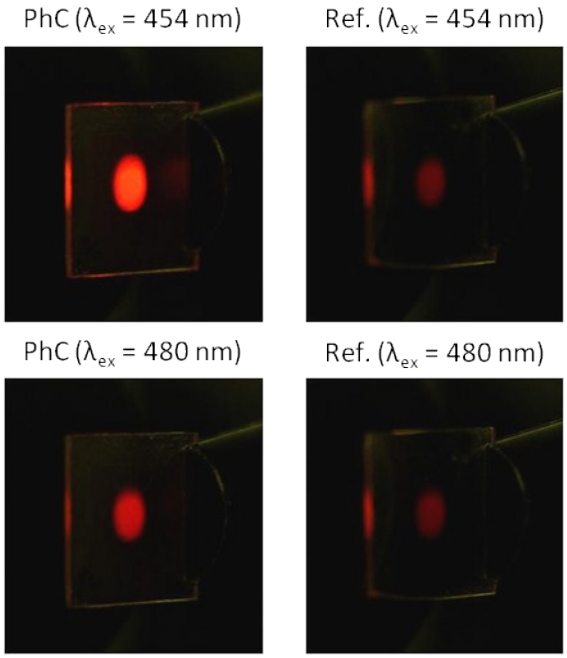

Fig. S3 CQD emission images at the emission resonance angle. All the images are taken at the emission resonance angle θ_{em} = 38°. The left and right columns correspond to the PhC and reference phosphors, respectively, while the top and bottom rows are for the excitation wavelengths of λ_{ex} = 454 nm (on-resonance) and λ_{ex} = 480 nm (off-resonance).

Optimization of the 1D PhC phosphor structure

In order to assess the maximum enhancement achievable by this approach, we attempted to optimize the 1D PhC phosphor structure. To be more specific, we investigated how the absorbance enhancement factor (with respect to the reference phosphor) depends on a couple of structural key parameters: thickness of the PhC phosphor slab, t, and CQD filling factor (FF). FDTD simulations were performed as done for Fig. 2c; for simplicity, however, here we assumed an ideal PhC phosphor structure with a planar (not groovy) CQD surface morphology (see Fig. S4a for the schematic). Shown in Fig. S4b is calculated absorbance enhancement factor as a function of slab thickness (t) and excitation wavelength (λ_{ex}); the period and the CQD filling factor were fixed at Λ = 300 nm and FF = 50%, respectively. Two local maxima, which correspond to ZC_1 and ZC_2, red-shift in excitation wavelength as the slab thickness increased. The absorbance enhancement factor reached its maximum (~15) when t = 130 nm (determined for ZC_2). It is interesting to note that this slab thickness corresponds approximately to $\lambda/2n_{\text{eff}}$, the condition for stable operation of the fundamental waveguide mode.

Now we examined the effect of the CQD filling factor. This time the period was kept the same as before (Λ = 300 nm), while the slab thickness was fixed at the optimum value, t = 130 nm. Fig. S4c shows the resultant absorbance enhancement factor as a function of the CQD filling factor over the range of 30-70%. We note that the two PBE modes, ZC_1 and ZC_2, react to the filling factor in opposite directions. Therefore, the filling factor of ~55%, at which the two curves for ZC_1 and ZC_2 cross over and the absorbance enhancement factor is about 10, may be considered optimum because the both PBEs are then equally useful at a compromised level. In fact, real applications circumstance where phosphor excitation is typically done by a broad

bandwidth source (much larger than the ~10 nm separation between the two PBE modes) would naturally let us choose the cross-over point.

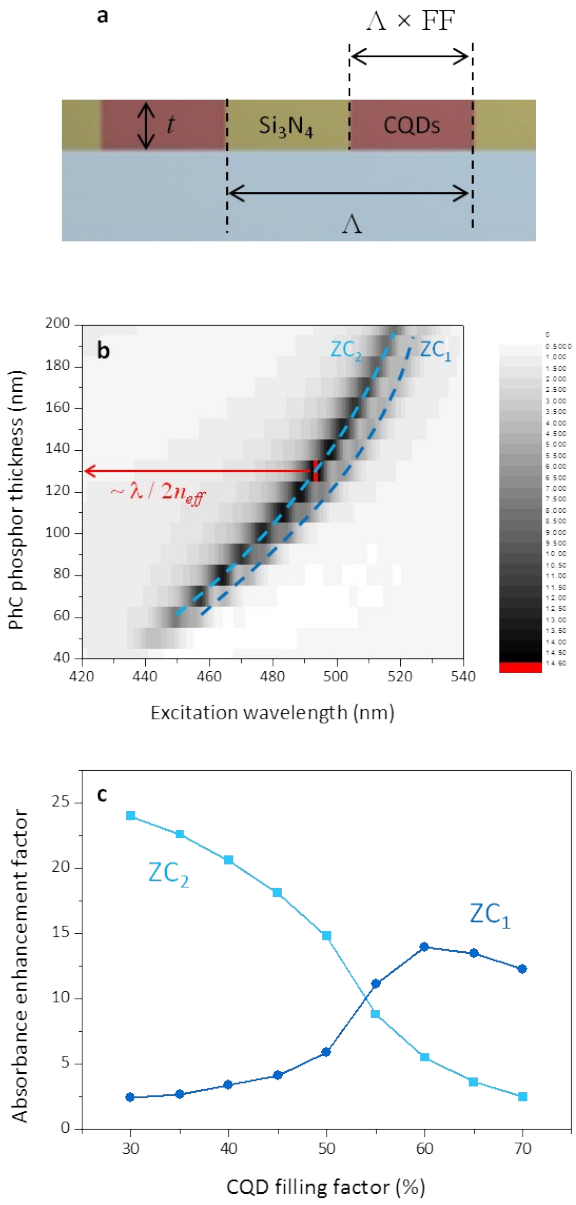

Fig. S4 Structural effects to the absorbance enhancement factor. (a) Schematic of an ideal 1D PhC phosphor structure. (b) Absorbance enhancement factor presented as a function of both excitation wavelength and slab waveguide thickness. (c) Absorbance enhancement factors calculated for the two PBE modes ZC_1 and ZC_2, both as functions of the CQD filling factor.

References

1. S. Fan, P. R. Villeneuve, J. D. Joannopoulos and E. F. Schubert, *Phys. Rev. Lett.*, 1997, **78**, 3294–3297.

2. J. J. Wierer Jr., A. David and M. M. Megens, *Nat. Photon.*, 2009, **3**, 163–169.